Appl. Phys. B 61, 585–592 (1995)

Applied Physics B Lasers and Optics

© Springer-Verlag 1995

Absolute concentration measurements of C_2 in a diamond CVD reactor by laser-induced fluorescence

C. Kaminski, P. Ewart

Clarendon Laboratory, Oxford University, Parks Road, Oxford OX1 3PU, UK
(Fax: + 44-865/272400, E-mail: EWARTGRP@uk.ac.ox.vax)

Received: 28 October 1994/Accepted: 3 February 1995

Abstract. By use of Laser-Induced Fluorescence (LIF) the absolute concentration of the C_2 radical in a microwave excited diamond chemical vapour deposition plasma has been measured for the first time. LIF spectra of the $d^3\Pi_g$–$a^3\Pi_u$ (1, 0) Swan band near 473 nm were recorded and synthesized theoretically allowing the plasma temperature of 2100 ± 200 K to be inferred. Quenching rates were determined from time-resolved measurements of the fluorescence decay. By calibrating the LIF detection system, using spontaneous Raman scattering in H_2 in the reactor vessel, the absolute concentration of C_2 was determined to be $(7.5 \pm 1.7) \times 10^{10}$ cm^{-3}. Observations of the C_2 density under varying plasma conditions are reported.

PACS: 07.65; 33.00

Low pressure microwave plasma Chemical Vapour Deposition (CVD) is a favoured technique for the production of high quality diamond films [1–4]. Although the quality of diamond films obtained with this method has constantly been improving in recent years, understanding of the fundamental chemical processes governing the deposition process is far from complete. One reason for this is the lack of experimental data which is required as input for chemical kinetics models. Theoretical models require detailed information of the concentrations of many chemical species present in the plasma environment. In particular one needs to know the spatial profiles and the variations of these concentrations as a function of parameter changes. Measuring the densities of many of the short-lived radicals important for diamond formation is a great experimental challenge. Their low densities and the extreme environment the plasma represents make their detection a difficult task.

This paper reports on what is believed to be the first quantitative measurement of C_2 concentrations in a low pressure diamond CVD reactor using Laser-Induced Fluorescence (LIF). C_2 is considered to be an important intermediate in the plasma environment [5] and has even been suggested as a possible growth species [6]. The importance of C_2 has recently been underlined by the observation that there is a strong correlation between the quality of the diamond films obtained and the quantity of C_2 present in the plasma [7].

LIF is a powerful, non-intrusive diagnostic technique offering high sensitivity and spatial resolution for the detection of minor species in hostile environments [8]. It has been successfully applied to measure the concentrations of short-lived radicals such as OH, C_2 and CH in atmospheric pressure flames [9, 10].

In low pressure systems concentrations of stable species could be successfully quantified by creating a calibration signal involving a known density of the species. On the other hand, absolute concentrations of transient species, such as OH, have also been determined in low pressure flames by cross-calibrating the LIF signal with absorption measurements. Measurements of NO and OH in a low pressure methane air flame (30–120 Torr) using these two techniques have been reported [11].

For most short-lived species present in a low pressure plasma, absorption is far too small to be measured directly. In this case some independent means of calibrating the LIF signal must be employed. In the present work calibration was achieved by use of spontaneous Raman scattering in H_2 following the method of Bischel [12].

1 LIF concentration measurements

In LIF, population is transferred from a ground state to an excited state during the laser pulse. The excited molecules relax to the available lower states. Some of these molecular transitions result in the emission of fluorescence photons. This induced fluorescence constitutes the LIF signal and is collected with a suitable light detection system. The number of photons emitted may be related to the population density of the absorbing species. For a quantitative measurement one has to take account of molecular collisions which can lead to population transfer back to the ground state without fluorescence being

emitted (quenching). It is equally important to know the efficiency of the fluorescence collection system and a calibration experiment is required to relate the LIF signal to an absolute number of photons emitted from the interaction region.

Quenching effects can in principle be overcome by using saturated LIF where the signal becomes independent of both laser power and collisions. However, proper application of this technique is very difficult because equal degrees of saturation cannot be achieved at all points of the interaction volume. For the present work it was decided to work in the unsaturated regime where the LIF signal is linear with laser energy. This requires knowledge of the quenching rates which were measured directly under similar experimental conditions.

Several methods have been employed for calibration of a fluorescence collection system. In one method laser light of the same wavelength as the LIF signal is scattered off a ground quartz disk placed at the interaction region. The interaction region is imaged by the same light collection system as the LIF signals and the same detection electronics are employed [13]. The signal thus created can be related to an absolute number of photons originating from the quartz disk. A problem with this method is that it is very difficult to relate the scattering geometry to the interaction volume of the corresponding LIF experiment.

A different method employs spontaneous Rayleigh scattering at the LIF emission wavelength created in a known concentration of a species with a known scattering cross-section [14, 15]. Here the interaction geometries match very well. However, the Rayleigh signal occurs at the laser wavelength and discrimination against laser scatter from windows and optical components is often not possible.

Bischel et al. [12] devised a calibration technique that is very similar in nature to the Rayleigh technique but is based on spontaneous Raman scattering in H_2. It offers the advantages of the former method with the additional advantage that the laser and signal wavelengths are well separated. Discrimination of the Raman signal is thus easily achieved. The spectroscopy of H_2 is very well understood and the Raman cross-sections for this molecule are accurately known. For these reasons spontaneous Raman scattering was an ideal candidate for accurate calibration of the LIF experiments described in this paper. Prior to a concentration measurement the reactor was simply filled with a few hundred Torr of room temperature H_2. The dye laser was retuned to the appropriate shorter wavelength to produce a Raman signal at the LIF emission wavelength. Beam geometry and detection system were exactly matched to the corresponding LIF experiment. The Raman signals were observed as a function of H_2 pressure and the resulting graph led to a calibration constant from which a LIF signal could be related to an absolute number of photons emitted from the interaction region.

2 Theory

The number of molecules N_2 transferred into the excited state during a laser pulse is given by [16]

$$N_2 = N_{10} \frac{B_{12}}{B_{12} + B_{21}} \frac{1}{1 + I_{sat}/I_\nu}, \tag{1}$$

where N_{10} is the ground state population prior to excitation by the laser pulse. B_{12} and B_{21} are the Einstein coefficients for stimulated absorption and stimulated emission respectively. I_ν is the spectral laser intensity (in W cm^{-2} Hz^{-1}) and the saturation intensity I_{sat} is defined as

$$I_{sat} = \frac{(A_{21} + Q_{21})c}{B_{12} + B_{21}}, \tag{2}$$

where A_{21} is the rate of spontaneous emission and Q_{21} is the collision-induced quenching rate. Equation (1) assumes that the system has reached steady state during the laser pulse. In saturated LIF one operates at $I_\nu \gg I_{sat}$. In this regime N_2 becomes independent of both laser power and quenching effects [17]. It can be seen that the fluorescence signal is a maximum at saturation. For these reasons saturated LIF is a useful technique for radical concentration measurements [18, 19]. However, several authors have pointed out pitfalls that can lead to large errors in concentration measurements when using saturated LIF. Complete spatial saturation cannot be achieved because of the intensity variation across the laser beam: in the wings of the laser beam profile the laser intensity falls off and quenching effects cannot be neglected in these regions [13]. Several models have been developed to account for these effects [20]. The spatial variation of the degree of saturation affects the local population dynamics and different rate equations may apply at different points within the interaction volume. The result is that temporal saturation may not occur simultaneously in all regions of the probe volume [21]. Neglect of these wing effects can lead to errors an order of magnitude larger than the measured concentration [22]. A method to eliminate the contributions from the lateral regions of the probe volume has been suggested by Salmon and Laurendau [15]. This method uses only the saturated fluorescence emitted along the axis of the laser beam. For a radially symmetric intensity profile this centre line fluorescence can be extracted from the lateral fluorescence profile by use of an Abel transformation [23]. The lateral profile of the fluorescence volume can be measured by scanning the image of the fluorescence volume across a narrow slit placed in the image plane of the fluorescence collection system. Since a large fraction of the signal is lost in this method high signal levels are needed to allow quantitative measurements with this technique.

In the present work I_ν was below or only slightly above I_{sat} to avoid the wing effects described above. Work in this regime requires knowledge of the quenching rate Q_{21}. A disadvantage is that errors in Q_{21} are carried over linearly into the concentration determination. This is the major reason why saturated LIF is the preferred method in atmospheric pressure application where quenching collisions dominate the population dynamics and cannot be measured directly [9]. However, the microwave plasma operates at moderate pressures (between 40 and 80 Torr) and this makes it possible to measure the decay rate of the fluorescence signal from which Q_{21} is obtained. Typical fluorescence decay times in the plasma were between 20 and 30 ns and could be determined to better than 1.5 ns.

The disadvantage of lower signal levels compared to saturated LIF, however, remains. Note that, in the present environment, I_{sat} for C_2 is only about 10^{-8} W cm^{-2} Hz^{-1} and great care has to be taken to avoid saturation.

The integrated signal S_{fl}, in volts per laser pulse, is given by

$$S_{fl} = \frac{N_2 A_\ell \theta_{fl}}{4\pi} D_{det} . \tag{3}$$

Here N_2 is the absolute number density of excited molecules present, θ_{fl} is the fluorescence quantum yield, and A_ℓ is the cross-sectional area of the laser beam in the interaction region. D_{det} is an overall system constant that is related to the efficiency of the detection system. It includes parameters such as photomultiplier gain, collection solid angle, interference filter bandpass function, and the length of the interaction volume imaged. D_{det} can be determined from a calibration measurement as outlined in the introduction.

In a two-level system the fluorescence quantum yield θ_{fl} is defined as

$$\theta_{fl} = \frac{A_{21}}{A_{21} + Q_{21}} , \tag{4}$$

where Q_{21} is the rate of quenching from the excited to the lower state.

D_{det}, used in combination with (3), allows determination of the number of excited molecules created in the interaction region imaged by the light collection system.

The integrated calibration signal from the spontaneous Raman scattering from H_2, measured in volts, using the same detection electronics as for the fluorescence experiment is given by [24]

$$S_{Ram} = \frac{E_0}{h\nu_s} N_0 \frac{\overline{\partial\theta}}{\partial\Omega} D_{det} . \tag{5}$$

Here E_0 is the pump laser energy, ν_s is the Stokes frequency, N_0 is the number density of the Raman active species and $\overline{\partial\theta/\partial\Omega}$ is the Raman cross-section averaged over the collection solid angle. S_{Ram} is linear in both number density and laser energy. From the slope of a plot of S_{Ram} against $E_0 N_0$ the calibration constant of the detection system D_{det} is found.

N_2 is determined from a LIF measurement and use of (3). N_2 is then related to the ground state population by use of (1). Finally, the total number density N_{tot} is determined from the respective Boltzmann fractions [25]:

$$N_{10} = \frac{N_{tot}}{Q_r} g_J \exp -(E_{rot}/k_B T). \tag{6}$$

J is the rotational quantum number, $g_J = (2J + 1)$ represents the degeneracy of the rotational state and E_{rot} is the energy of the rotational level concerned. Q_r is the rotational state sum of the system under investigation [25]. Equation (6) requires knowledge of the temperature of the system which may also be determined by LIF. For this purpose the dye laser frequency is scanned over the individual rotational transitions of the molecule. The relative intensities corresponding to the resulting fluorescence peaks are proportional to the relative concentrations of the individual rotational states. From the measured intensities and knowledge of rotational line strengths the fractional populations in each rotational level can be determined [26]. Since the rotational state population follows a Boltzmann distribution the fractional populations can be related to a temperature from a Boltzmann plot. The gradient of a plot of $\ln(N_i/g_i)$ vs E_i, where N_i is the population, g_i the degeneracy and E_i the energy of level i respectively, yields the temperature of the system.

The method employed in this work was to fit a synthesized spectrum directly to the measured spectrum and this will be discussed in more detail in Sect. 4.

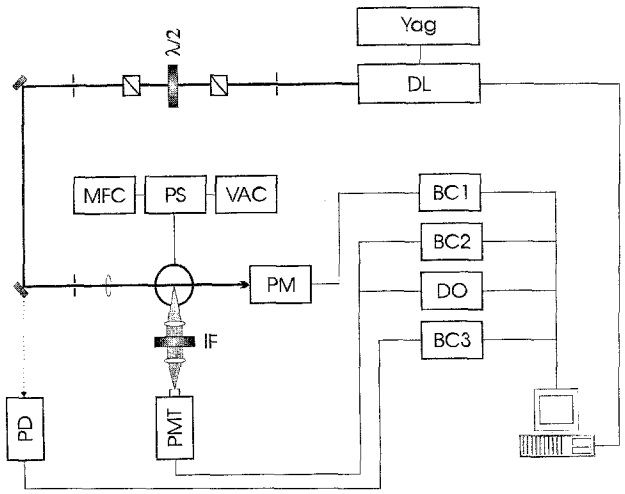

Fig. 1. Experimental setup for LIF and Raman experiments (DL, dye laser; $\lambda/2$: half-wave plate; MFC: mass flow controllers; PS: pressure sensor; VAC: vacuum system; PD: photodiode; PMT: photomultiplier tube; PM: power meter; IF: interference filter; BC1, 2, 3: boxcar integrator channels 1, 2, 3; DO: digital oscilloscope)

3 Experimental method

The system used in this experiment was a low pressure microwave-assisted diamond CVD reactor. It consisted of a stainless steel reactor with four optical windows allowing access to the region above the substrate surface. The substrate was a 2 inch polished silicon disk of 3 mm thickness and its position could be translated vertically via the adjustable substrate table. The feedstock gases used were H_2, Ar and CH_4. Typical flows were 800 sccm (standard cubic centimeters per minute) H_2, 40 sccm CH_4 and 500 sccm of Ar at total pressures between 50 and 100 Torr. Pressures and flows were monitored by a feedback controlled vacuum system and precision mass flow controllers respectively.

The apparatus for the LIF and Raman measurements is shown schematically in Fig. 1.

The laser system consisted of a Quanta Ray PDL-3 dye laser pumped by the third harmonic of a Spectron SL4000 Nd:YAG laser. For the LIF experiments in C_2, Coumarin 460 laser dye dissolved in methanol was used. The dye laser operated near 470 nm with a linewidth of 0.1 cm^{-1}. The pump energy was approximately 60 mJ giving around 6 mJ of dye laser output. The dye laser

beam was passed through a linear polarizer, allowed to propagate for 8 m and apertured to produce a very uniform beam profile in order to prevent the possibility of local saturation by "hot spots" within the beam. A calibrated half-wave plate (Laser Optics) – rotation stage assembly in front of a polarizer allowed the laser energy to be varied continuously without introducing beamwalk. For the concentration measurements pulse energies were between 5 and 50 μJ. The laser beam was focused by a 1 m focal length lens resulting in a measured beam area of 0.8 mm^2 at the interaction region. The beam passed onto a calibrated energy meter (Scientech 365 or Scientech 362) corrected for reflection losses at the exit window. Additionally, laser energies were monitored on a silicon photodiode picking up leakage behind a beam steering mirror. Both fluorescence and Raman signals were imaged by an approximately *f*/8 optical system (essentially determined by the size of the reactor windows) onto a 1 mm diameter aperture placed 3 cm in front of a Thorn EMI 9783B electron photomultiplier tube. Stray light and window scatter were effectively suppressed by a 10 nm bandwidth interference filter, centred on 510 nm, which is close to the head of the C_2 (1, 1) Swan band where most of the fluorescence emission occurs. Signals from photomultiplier, energy meter and photodiode were collected by a three channel boxcar integrator (Stanford Research SR250) and transferred to a laboratory computer for storage and processing.

For C_2 the ($\Delta v = 1$) transitions in the $d^3\Pi_g$–$a^3\Pi_u$ Swan system at around 473 nm were excited [27]. Most of the induced fluorescence is subsequently emitted in the (1, 1) band and some in the (0, 0) band at 511 and 516 nm respectively.

For measurements of quenching rates, a digital sampling oscilloscope (Hewlett-Packard 54510A) having a time resolution of 1 ns was used to resolve the LIF signals from the photomultiplier tube which had a rise time of less than 3 ns. The LIF signals from a particular transition were averaged over 512 shots. The data were directly fitted with exponential decay curves from which the quenching rates could be determined [28].

For the calibration measurements using spontaneous Raman scattering, the reactor was filled to pressures up to 700 Torr of H_2 as recorded by a calibrated capacitance manometer. The laser was operated at 421 nm to produce a Raman signal at 511 nm which was thus closely matched to the region of the maximum fluorescence in C_2. For this purpose the Coumarin dye was changed to Exalite 428 (Exciton) dissolved in dioxane. The dye laser produced 7 mJ per pulse at 421 nm. The laser beam was allowed to propagate through exactly the same 8 m path and the series of apertures which defined the LIF geometry. In this way the beam cross-section and the imaged interaction volume were ensured to be the same for both the LIF and Raman signals. The Raman shift of 4155 cm^{-1} arises from the H_2 Q-branch vibrational transition. Most of the ground state population (66%) in H_2 at room temperature is in the $J = 1$ state. For this reason the $Q(1)$ Raman line at 4155 cm^{-1} produces the strongest contribution to the Raman signal [29].

The pulse energies were attenuated to yield between 0.15 and 2 mJ in the interaction region. Care was taken to ensure the detection electronics and signal collection system were the same as for the corresponding LIF measurement. It was verified that the observed signals arose from Raman scattering in H_2 (and not from "leaked" Rayleigh scattering which is orders of magnitude more efficient than Raman scattering) by filling the chamber with 1 atm of argon. No signals were observed in this case.

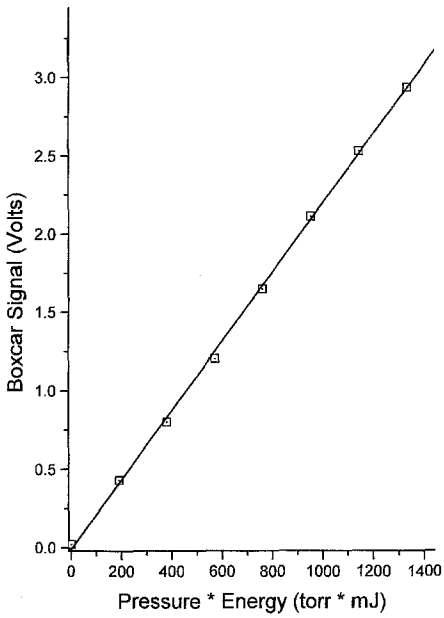

Fig. 2. Spontaneous Raman calibration graph exhibiting linearity of the spontaneous Raman signal in both laser energy and H_2 pressure. A linear fit yields a slope of 2.21 $mV\,mJ^{-1}\,Torr^{-1}$. This particular measurement yielded a LIF calibration constant $D_{det} = 8.98 \times 10^{-6}$ Vcm sr

4 Results and discussion

4.1 Calibration using spontaneous Raman scattering

Figure 2 shows a typical result for a spontaneous Raman scattering measurement. The signal is plotted as a function of hydrogen pressure and laser energy. For this particular measurement the pulse energy was kept constant at 1.9 mJ and the H_2 pressure varied between 0 and 700 Torr. Pressure changes were made in 100 Torr steps and signals were averaged over 1000 shots per point. A linear fit through these points gives a slope of 2.21 $mV\,mJ^{-1}\,Torr^{-1}$. The calibration constant D_{det} could now be determined from (5). The hydrogen number density N_0 was calculated using the ideal gas law at room temperature. To calculate the H_2 Raman scattering cross-section at a pump wavelength of 421 nm the empirical formula given in [12] was employed. This gives a value for an infinitesimal collection solid angle in a direction that is perpendicular to both the laser axis and the laser polarization (i.e., vertically polarized laser light). Depolarization effects are accounted for by averaging the cross-section over the collection solid angle of the imaging system [30, 24]. For the small collection solid angle in the present experiments depolarization effects were negligible

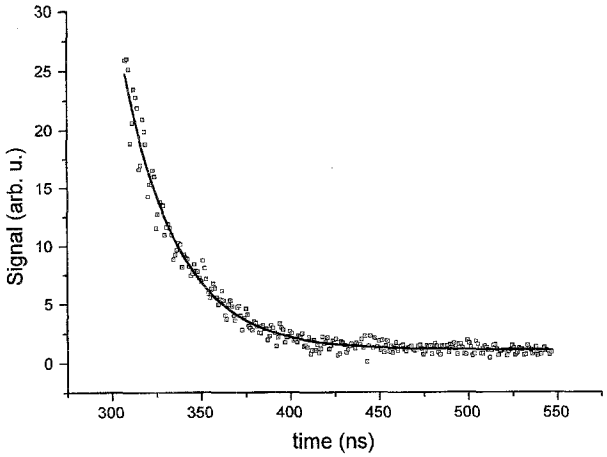

Fig. 3. LIF signal decay. Exponential fit to the LIF signal at 65.1 Torr. The fit yields a time constant $\tau_{fl} = 30$ ns corresponding to a fluorescence quantum yield $\theta_{fl} = 0.25$

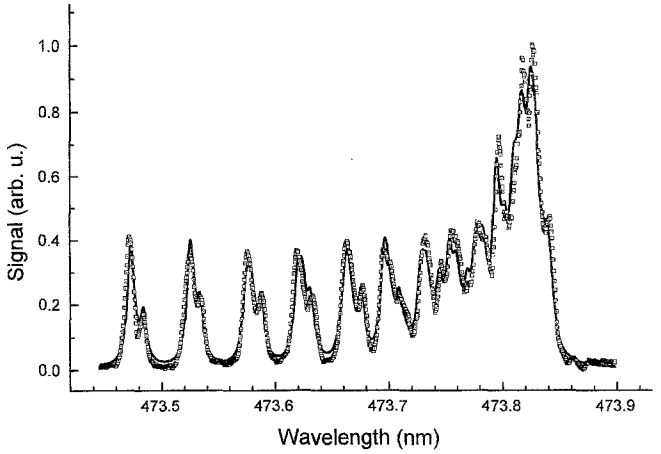

Fig. 4. LIF temperature determination. LIF spectrum of *P*-branch of the $d\ ^3\Pi_g(\Delta v = 1) \rightarrow a\ ^3\Pi_u(\Delta v = 0)$ Swan band in C_2. The *solid line* is a theoretical fit to the data corresponding to a temperature of 2100 K

and so in (5) the differential scattering cross-section is given by

$$\overline{\frac{\partial \theta}{\partial \Omega}} = \frac{\partial \theta}{\partial \Omega}(90°). \tag{7}$$

At 421 nm pump light a H_2 Raman scattering cross-section of 2.93×10^{-30} $cm^2 sr^{-1}$ is obtained. Hence from (5), $D_{det} = 8.98 \times 10^{-6}$ Vcmsr.

The Raman signals were very reproducible for a given setup of the light detection system. The linear energy dependence of the Raman signal was verified by filling the chamber with a constant H_2 pressure of 700 Torr and varying the pulse energy using the wave plate–polarizer assembly. The slopes obtained for this arrangement were identical to the ones obtained in the former case in which the laser energy was kept constant and the pressure varied.

4.2 Quenching measurements

The decay of the fluorescence signal is shown in Fig. 3, obtained by averaging the LIF signal over 512 laser shots and corrected for background and electrical noise. The data points between 5 and 95% of the maximum signal level are used to ensure that the signal was being sampled only after the laser pulse had decayed. The exponential fit shown in Fig. 3 yields a fluorescence signal time constant τ_{fl} of 30 ns. Here τ_{fl} is defined as [28]

$$\tau_{fl} = \frac{1}{Q_{21} + A_{21}}. \tag{8}$$

Determination of the fluorescence quantum yield θ_{fl} requires knowledge of the radiative rate A_{21}. In principle this can be obtained by extrapolation of measured decay times to zero pressure. This method yielded a radiative lifetime of $\tau_r = 170$ ns. However, this value was not applied to determine the radiative rate for the following reasons: The pressure of the system could be varied only between 50 and 100 Torr for stable plasma operation and so only very few points were available for the extrapolation. The system took a very long time to reach a stable state (typically 30 min following a change to the pressure or the flow rate). Finally, the temperatures of the plasma are quite different for different pressures. The chemistry inside the plasma is extremely sensitive to temperature changes [2] and therefore a linear dependence of the quenching rate with pressure cannot be tacitly assumed. Although there remains some uncertainty about the absolute value of τ_r for the $d^3\Pi_g$–$a^3\Pi_u$ transition in C_2 [9], recent measurements suggest a value of $\tau_r = 120$ ns [31]. For a total pressure of 65 Torr with 824 sccm of H_2, 65 sccm of CH_4, 525 sccm of Ar and a microwave power of 800 W the fluorescence quantum yield obtained was $\theta_{fl} = 0.25$.

4.3 Temperature determination

The temperatures for the Boltzmann fractions (6) were determined by scanning the laser across the *P*-branch of the $d^3\Pi_g$–$a^3\Pi_u$ (1,0) transition which forms the head of the $\Delta v = 1$ Swan band. The direct spectrum fitting method employed in this work has the advantage that complex overlapping spectra can be modelled [32]. The alternative approach described in Sect. 2 is to plot a Boltzmann graph whose slope yields the temperature of the system. This method requires isolated rotational lines. Unfortunately C_2 spectra are quite crowded and many of the rotational lines were not individually resolved making this method difficult to apply.

The large bandwidth of the detection system employed (~ 10 nm) ensured that transmission was constant over the spectral region scanned by the dye laser (~ 0.5 nm). Spectral bias of the collection system can have large effects on the accuracy of temperature determinations and is discussed in detail in [32]. Collisional effects were assumed to be constant for the different rotational levels in this low pressure system [33]. Figure 4 shows a spectrum obtained for the conditions referred to above. Each data

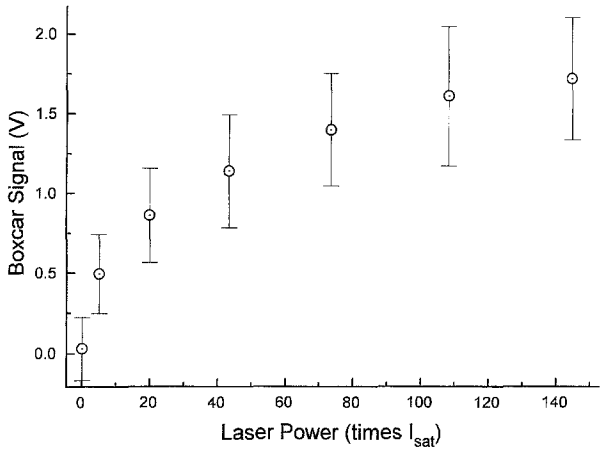

Fig. 5. LIF saturation behaviour. LIF signal behaviour over a large range of laser intensities. The laser intensity is expressed in terms of I_{sat} which is defined by (2). Note the increase of the LIF signal even for intensities much greater than I_{sat}

point represents the average over 30 laser shots. The resulting spectrum was directly fitted with synthesized spectra using a NAG minimization routine (NAG E04JAF) to find the least-squares fit to the experimental spectrum. The spectra were synthesized using Lorentzian lineshapes centred on line positions taken from [34, 35]. The linewidths are not determined by laser saturation but are thought to be dominated by Stark-induced dephasing processes present in the microwave plasma. The Hoenl-London factors were calculated from the formulae first derived by Budó [36] which assume Hund's case (b) coupling. This limit is rapidly approached for higher J values [37]. The spectrum shows the P-branch for J values between 0 and 33. The fit gives a temperature of 2100 ± 200 K.

4.4 Concentration determination

For the concentration measurements we excite a line which consists of the overlapping F_2 ($J = 21$) and F_2 ($J = 12$) transitions (notation follows [34]). Plots of LIF signal vs laser intensity exhibited linear behaviour for small intensities and started to roll over as I_v approached I_{sat}. This gave confidence that the fluorescence collection volume sampled was very similar to the unsaturated Raman signal. Figure 5 shows the saturation behaviour for a large range of intensities. Note that even at very high intensities with $I_v \gg I_{sat}$ the LIF signal still increases. Linear behaviour is exhibited only very close to the origin. This arises from the increased lateral extent of the fluorescence volume being sampled at high intensities. To verify this behaviour the 1 mm pinhole in front of the PMT was replaced with a 50 μm slit aligned parallel to the laser axis. The PMT was translated vertically on a micrometer stage and this allowed sampling of the fluorescence volume at different heights. This experiment showed that at very high intensities ($I_v \sim 50 I_{sat}$) the lateral extent of the fluorescence volume was more than three times greater than the corresponding Raman volume. With such lateral profile measurements it is possible, in principle, to extract the centre line fluorescence emission which allows quantitative measurements using saturated LIF [15]. This approach was not attempted here.

The concentration measurements presented in this paper were conducted at 65 Torr total pressure with respective flows of 824 sccm H_2, 65 sccm CH_4, and 524 sccm of Ar. The microwave input power was 800 W. From the quenching measurements the fluorescence quantum yield was measured to be 0.25 for this environment. Using $D_{det} = 8.98 \times 10^{-6}$ Vcm sr and $A_\ell = 0.8$ mm^2 with (5) and (3) the density of excited molecules was calculated to be 1.68×10^9 cm^{-3}. Equation (1) yields a ground state density of $N_{10} = 4.0 \times 10^9$ cm^{-3} corresponding to a measured $I_v = 5 I_{sat}$. From (6) the total number density could now be calculated. Since the LIF signal arises from the overlapping F_2 ($J = 21$) and F_2 ($J = 12$) transitions, calculation of both Boltzmann fractions is required. Since the laser linewidth is much smaller than the transition width of the individual lines the measured intensity is the sum of their individual intensities. The rotational energy E_{rot} in (6) was evaluated by approximating

$$E_{rot} = BhcJ(J + 1). \tag{9}$$

The rotational constant B for C_2 in (9) was taken from [38]. Substituting a measured temperature of $T = 2100$ K the final concentration obtained is 7.53×10^{10} cm^{-3}.

4.5 Experimental uncertainties

Errors in the determination of N_2 arise from uncertainties in D_{det}, the fluorescence quantum yield θ_{fl}, the measured cross-sectional area of the laser beam A_ℓ, and the signal level S_{fl}. D_{det} was determined directly from the slope of the H_2 Raman signal as a function of laser energy and pressure, all of which could be measured to better than 1%. The Raman signals were very reproducible for a given experimental setup and the slopes obtained agreed to within 1%. A larger error is associated with θ_{fl}. Lifetimes, τ_{fl}, obtained for a given plasma environment agreed to within 4% and this was the error associated with θ_{fl}.

The interaction region was a long distance in front of the focal region of the laser beam and hence A_ℓ could be calculated using a simple geometrical formula. An error of 3% was associated with this calculation. Errors in the measured fluorescence signal S_{fl} were negligible (S/N ratio of $> 100:1$).

Measurement of the ground state density required knowledge of I_v (1). The laser energy per pulse was determined with the calibrated half-wave plate / polarizer assembly. Dye laser pulse lengths were measured to be 6.4 ns on the sampling oscilloscope using a fast photodiode (Thorlabs DET2-SI). The time-averaged linewidth of the laser was measured using an etalon having a free spectral range of 1 cm^{-1} by scanning the laser to generate a "centre spot" fringe pattern. The profiles recorded using a boxcar averager were fitted with Lorentzians (Fig. 6) from which a linewidth of 3.75 GHz was determined. The combined uncertainties of these measurements resulted in a 6% error associated with I_v.

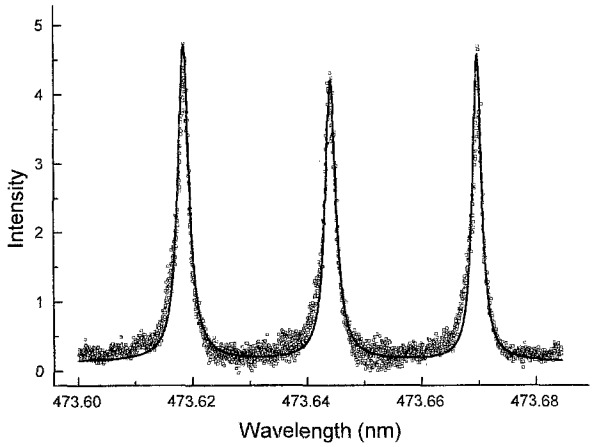

Fig. 6. Dye laser linewidth measurements. Fabry Perot etalon fringes for the dye laser. The Lorentzian lineshapes correspond to a laser linewidth of 3.75 GHz

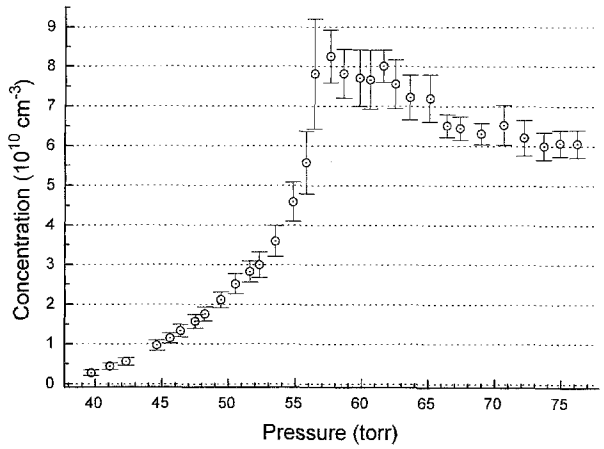

Fig. 7. C_2 concentrations as a function of overall gas pressure

Finally the $\pm$ 200 K uncertainty associated with the temperature measurement at 2100 K resulted in a 7% error of the Boltzmann fractions. Combining these errors the total number density can be quoted as $N_{tot} = (7.5 \pm 1.7) \times 10^{10}$ cm^{-3}. The stated error reflects only imprecisions of the present measurement. In addition there will be uncertainties associated with the range of values for $\partial\theta/\partial\Omega$, B, τ_r quoted in the literature. The combined effect of these is estimated to be less than 5%. Much of the error quoted in the final concentration stems from the uncertainty in the temperature measurement which arises from the relative insensitivity of the C_2 LIF spectra to temperature changes. Independent, more accurate thermometric techniques (for example coherent anti-Stokes Raman scattering in H_2) would reduce the final error.

4.6 Concentrations in various plasma environments

Figure 7 shows the C_2 concentration in the plasma ball for total gas pressures between 40 and 80 Torr. The measurement sampled the plasma at a position 12 mm above the substrate surface. In principle each data point on the graph would require a different measurement of Q_{21} and θ_{fl}. However, over the pressure range indicated the fluorescence lifetime τ_{fl} (and hence θ_{fl}) did not change by more than 10%. Supposing a temperature range from 1500 to 3000 K was associated with this pressure range, (6) would introduce a maximal uncertainty of 35% in the number density. Although temperatures in the plasma are sensitive to pressure changes, temperature measurements conducted at different pressures indicate a much smaller temperature variation than this. For example, temperature measurements carried out at 53 and 69 Torr yielded temperatures of 1950 $\pm$ 200 and 2100 $\pm$ 200 K, respectively.

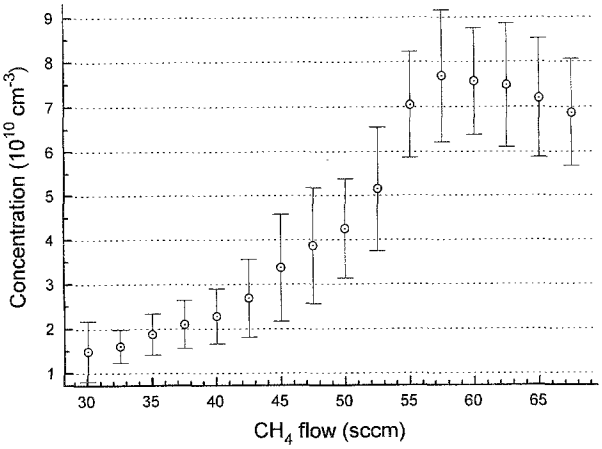

Fig. 8. C_2 concentrations as a function of methane flow

Figure 7 is simply a plot of the relative LIF signal strength as a function of total pressure referenced to an absolute concentration measurement conducted at 65.1 Torr. The origin of the graph was obtained by switching off the methane flow after which the LIF signal disappeared completely. Each data point on the graph represents the signal average corresponding to 1000 laser shots. Note the steep rise in the C_2 concentration to a maximum at 57.5 Torr and the gradual fall off at higher pressures. Note also the LIF detection sensitivity, allowing concentrations to be measured down to a few tens of ppb.

In Fig. 8, the C_2 concentration is shown as a function of methane flow. The measurements were taken at a constant total pressure of 65.1 Torr. Again a signal peak is observed corresponding to a flow of 58 sccm. No attempt was made to model the behaviour of C_2 concentrations in the present work. In Fig. 9, the sensitivity of the C_2 concentration to changes in microwave power is shown. The sharp rise above 770 W is indicative of the sensitivity of the chemistry inside the plasma to small parameter changes. Such data may prove useful not only from a theoretical modeller's point of view but they may also be beneficial from a practical viewpoint: the conditions inside the plasma may be correlated to the properties of the diamond film produced. This provides a tool to control the deposition process and may be used to optimize growth to achieve particular film characteristics. The present study was designed to determine the feasibility of quantitative diagnostic techniques for absolute

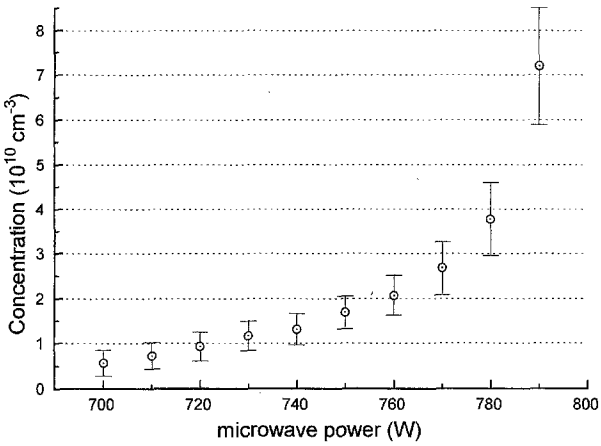

Fig. 9. C_2 concentrations as a function of microwave power

concentration measurements and no attempt was made to assess the quality or quantity of any diamond grown. Investigations are currently under way to probe the chemically interesting boundary layer immediately above the substrate surface. Spatially resolved concentration measurements of the boundary layer are of great interest to modellers. Unfortunately optical access to this region is very restricted in the current reactor system. Preliminary studies have been conducted by translating the substrate table within the reactor chamber but this method is not justified for quantitative measurements since changes of the substrate position influence the plasma characteristics substantially.

5 Conclusion

This work reports on what is believed to be first quantitative measurement of C_2 concentrations in a low pressure microwave-assisted diamond CVD reactor using laser-induced fluorescence. The high spatial resolution and sensitivity afforded by LIF make it an ideal tool for in situ detection and non-intrusive monitoring of radical species important in CVD diamond growth.

Spontaneous Raman scattering in H_2 was used in this work to calibrate the fluorescence collection system absolutely. Great care was taken to ensure that the LIF calibration was not affected by "wing effects" associated with saturation. The C_2 concentration profiles presented in this work highlight the great sensitivity of the chemistry inside the plasma to small parameter changes. Such concentration profiles can thus be used for detailed comparisons with computer calculations modelling the plasma environment.

Future work will focus on the application of the present technique to obtain concentration profiles of other trace species present in the plasma. In particular, concentration profiles of CH will be assessed. Presently efforts are aimed at "mapping" of species concentrations as a function of position inside the chemical boundary layer close to the substrate surface.

Acknowledgement. The authors would like to thank Dr. I. Hughes for many useful discussions and comments.

References

1. J.C. Angus, C.C. Hayman: Science **241**, 913 (1988)
2. F.G. Celii, J.E. Butler: Ann. Rev. Phys. Chem. **42**, 643 (1991)
3. P.K. Bachmann, R. Messler: Chem. Eng. **67**, 24 (1989)
4. P.K. Bachmann, W.D. Drawl, R. Weimer, R.F. Messier: *Diamond and Diamond-like Materials Synthesis* (Materials Research Society, Pittsburgh, PA 1988) Extended Abstracts, No. 15
5. Y. Matsui, A. Yuuki, M. Sahara, Y. Hirose: Jpn. J. Appl. Phys. **28**, 1718 (1989)
6. T. Yasuda, K. Miyamoto, M. Ihara, H. Komiyama: In *New Diamond Science and Technology*, Mater. Res. Soc. Symp. Int'l Proc. NDST-2 (Materials Research Society, Pittsburgh, PA 1991)
7. G. Balestrino, M. Marinelli, A. Paoletti, I. Pinter, A. Tebano: Appl. Phys. Lett. **62**, 879 (1993)
8. D.R. Crosley, G.P. Smith: Opt. Eng. **22**, 545 (1983)
9. A.P. Baronavski, J.R. McDonald: Appl. Opt. **16**, 1897 (1977)
10. K.C. Smyth, P.J.H. Tjossem: Appl. Phys. B **50**, 499 (1990)
11. D.E. Heard, J.B. Jeffries, G.P. Smith, D.R. Crosley: Combust. Flame **88**, 137 (1992)
12. W.K. Bischel, D.J. Bamford, L.E. Jusinski: Appl. Opt. **25**, 1215 (1986)
13. K. Kohse Höinghaus, W. Perc, Th. Just: Ber. Bunsenges. Phys. Chem. **87**, 1052 (1983)
14. P.A. Bonczyk, J.A. Shirley: Combust. Flame **34**, 253 (1979)
15. J.T. Salmon, N.M. Laurendau: Appl. Opt. **24**, 6 (1985)
16. A.C. Eckbreth: *Laser Diagnostics for Combustion Temperature and Species*, Energy Eng. Sci. Ser., Vol. 7 (Abacus, Tunbridge Wells, UK 1988)
17. E.H. Piepmeier: Spectrochim. Acta **27B**, 431 (1972)
18. M. Mailänder: J. Appl. Phys. **49**, 1257 (1978)
19. J.W. Daily: Appl. Opt. **16**, 568 (1977)
20. J.W. Daily: Appl. Opt. **17**, 225 (1978)
21. J.T. Salmon, N.M. Laurendau: Appl. Opt. **24**, 1313 (1985)
22. A.D. Sappey, D.R. Crosley, R.A. Copeland: Appl. Phys. B **50**, 463 (1990)
23. M.P. Freeman, S. Katz: J. Opt. Soc. Am. **53**, 1172 (1963)
24. H.W. Schrotter, H.W. Klockner: *Raman Scattering Cross Sections in Gases and Liquids* (Springer, Berlin, Heidelberg 1979)
25. G. Herzberg: *Spectra of Diatomic Molecules*, Molecular Spectra and Molecular Structure, Vol. 1 (Van Nostrand Reinhold, New York 1950)
26. D.R. Crosley, G.P. Smith: Combust. Flame **44**, 27 (1982)
27. D.L. Lambert, A.C. Danks: Astr. J. **268**, 428 (1983)
28. K.J. Rensberger, M.J. Dyer, A. Copeland: Appl. Opt. **27**, 17 (1988)
29. J.V. Foltz, D.H. Rank, T.A. Wiggins: J. Mol. Spectrosc. **21**, 203 (1966)
30. W. Holzer, Y. Le Duff, K. Altmann: J. Chem. Phys. **58**, 642 (1973)
31. L. Curtis, B. Engman, P. Erman: Phys. Scr. **13**, 270 (1976)
32. K.J. Rensberger, J.B. Jeffries, R.A. Copeland, K. Kohse-Höinghaus, M.L. Wise, D.R. Crosley: Appl. Opt. **28**, 3556 (1989)
33. D.R. Crosley: Opt. Eng. **20**, 511 (1981)
34. T. Suzuki, S. Saito, E. Hirota: J. Mol. Spectrosc. **113**, 399 (1985)
35. J.G. Phillips, S.P. Davis: *The Swan System of the C_2 Molecule*, Berkeley Atlas of Molecular Spectra (Univ. California Press, Berkeley, CA 1968)
36. A. Budó: Z. Phys. **96**, 219 (1935)
37. L.L. Danylewytch, R.W. Nicholls: Proc. R. Soc. London A **339**, 197 (1974)
38. K.P. Huber, G. Herzberg: *Constants of Diatomic Molecules* (Van Nostrand Reinhold, New York 1978)